Desalination and Water Treatment
www.deswater.com

doi: 10.1080/19443994.2015.1010275

57 (2016) 6633–6643
March

Taylor & Francis
Taylor & Francis Group

Closed circuit PRO series no 2: performance projections for PRO membranes based on actual/ideal flux ratio of forward osmosis

Avi Efraty

Osmotech Ltd, P.O. Box 132, Har Adar 90836, Israel, Tel. +972 52 4765 687; Fax: +972 2 570 0262; email: efraty.adt@012.net.il

Received 6 November 2014; Accepted 15 January 2015

ABSTRACT

Pressure retarded osmosis (PRO) for hydroelectric power generation from worldwide widespread salinity gradient sources is of growing interest for large-scale clean energy generation. This approach requires membranes of specific characteristic and the evaluation of peak power density of such membranes at present time proceeds by extrapolation from theoretical curves with limited experimental data support mostly in a region far removed from the actual applied pressure of peak power generation. This study describes the use of actual/ideal flux ratio term (β) derived from PRO flux measurement at zero applied pressure (forward osmosis flux conditions) in a distinct salinity gradient for a defined membrane of known permeability coefficient (A) for the flux and power density projections of said membrane. The β-A approach for PRO flux, power density, and peak power projections is illustrated in the context of some recently reported theoretical and experimental results of several advanced Thin Film Composite-PRO membranes.

Keywords: Pressure retarded osmosis (PRO); PRO peak power; Peak power projections of PRO membranes; PRO applied pressure at peak power; PRO for clean hydroelectric power generation

1. Introduction

In light of rapidly expanding global population, increased standards of living and enhanced utility of polluting fossil fuels, the need to develop large-scale viable clean energy technologies for widespread applications worldwide appears of high priority environmentally and economically. Conventional hydroelectric power generation is, at present time, the single largest source of clean power providing some 2.3% of the global power needs compared with less than 0.5% from other sources (e.g. wind, solar, biomass, geothermal, etc.). A newly emerging plausible technology for large-scale clean energy generation is the so-called pressure retarded osmosis (PRO) method, which was conceived by Loeb [1,2] in 1975, the same person which 15 years earlier conceived [3] the use of reverse osmosis (RO) for seawater and brackish water desalination. PRO is a membrane technology [4,5] for hydroelectric power generation from salinity gradients of worldwide abundance, such as rivers at their outlets into the sea or any other sources of different concentrations. When two streams of different salinity meet on the opposite sides of a semipermeable membrane, pressurized water permeation takes place toward the side of higher concentration by a natural forward osmosis (FO) process, which could be used for hydroelectric power generation as well as for other applications, including desalination [6]. PRO power

generation prospects depend on the magnitude of the salinity gradient as well as on the availability of suitable membranes and technology for such an application—aspects considered next.

1.1. Salinity gradient sources

Salinity gradient sources are the basic fuels of the PRO power generation technology with larger gradients concomitant with greater power output. Although the enormous osmotic pressure difference (~250 bar) between the Dead Sea (35%) and the Mediterranean Sea (4.0%) contributed to the inception of PRO by Loeb [7], the major efforts today are directed toward the salinity gradient systems SW-RW, SWB-RW, and SWB-BW; wherein, SW stands for seawater, SWB for seawater brine from SWRO desalination plants, and BW for low-salinity brackish water like sources, including such comprising treated domestic effluents. The Statkarft company [8–10] in Norway pioneered the efforts to develop PRO commercial applications for SW-RW-type gradient systems; whereas, the "Mega-ton Water System Porject" [11–13] in Japan focused on the development of commercial applications for SWB-BW-type gradient systems with some promising results already received. Very little attention has been given thus far to salinity gradient systems such as SW-SWB and SW-SWCEP; wherein, SWCEP stand for seawater concentrates in evaporation ponds of hundreds of salt productions factories worldwide, which could be used for PRO power generation apart from their traditional role.

1.2. Semi-permeable PRO membranes for hydroelectric power generation

Semi-permeable membranes for PRO applications should possess features, such as high permeability coefficients (A), sufficiently low salt diffusion coefficients (B), small structural parameters (S), and sufficiently high mechanical strength to withstand applied pressures of peak power density. Power density of PRO membranes (P, W/m^2) is expressed by Eq. (1); wherein, J_w stands for water flux (lmh) across the membrane, $\Delta\pi$ for osmotic pressure gradient (bar), and p_a (bar) for applied hydraulic pressure. Ideal water flux is expressed by Eq. (2); however, the reverse salt diffusion flux (J_s) expressed by Eq. (3) as a result of the concentration difference between the high salinity draw (C_D) and low salinity feed (C_F) solutions could not be ignored. The membrane support layer, which separates between the bulk concentrations creates a unique zone of different stationary state conditions, wherein, the effective feed concentration at the active TFC (thin-film composite) layer (C_{F-E}) is higher than that in the bulk ($C_{F-E} > C_F$) and therefore, the effective osmotic pressure difference across the active membrane layer ($\Delta\pi_m$) is lower than that between the bulk solutions ($\Delta\pi_m < \Delta\pi$), and this will prompt a lower effective net driving pressure across the active layer (AL) ($\Delta\pi_m - p_a$), causing a lower PRO power output. The effects created in the porous support layer on PRO power generation, the so-called internal concentration polarization (ICP) effects, are functions of A, B, and the structural parameter S, defined by Eq. (4); wherein, t_s stands for the support thickness, τ for the support tortuosity, and ε for the support porosity. The S parameter expresses the distance, which a solute particle needs to pass from the AL to the bulk of the feed solution. The detrimental effects on the power availability of PRO membranes are well understood today, in terms of ICP, external concentrations polarization and structural parameters arising from the intrinsic characteristic features A, B, and S of membranes.

$$P = (1/36) \times J_w \times p_a \tag{1}$$

$$J_w = A \times (\Delta\pi - p_a) \tag{2}$$

$$J_s = B \times (C_D - C_F) \tag{3}$$

$$S = t_s \times \tau/\varepsilon \tag{4}$$

The increased awareness of PRO as a major prospective source for clean hydroelectric power generation has led to a rapid growth of noteworthy reports [14–24] on advanced TFC-PRO membranes. These reports describe the fabrication of new advanced flat sheet and hollow fiber PRO membranes of stronger support, and more effective AL and their characteristic features (e.g. A, B, S, etc.), and mechanical properties to withstand applied hydraulic pressure. Many of these studies also contain comprehensive theoretical model analyses with A, B, and S parameters used for actual flux and power density projections of specific membranes in defined salinity gradients. Theoretical projections require experimental validations, and the combined theoretical–experimental approach constitutes a powerful tool in the development of better more effective PRO membranes. The lengthy experimental–theoretical procedure for performance evaluation of newly fabricated PRO membranes may suggest the need for a simple and quick procedure for such a purpose and such a procedure is described by this study.

1.3. PRO hydroelectric power generation methods

The conceptual approach of the conventional PRO technology conceived by Loeb [1–3] requires the engagement of an energy recovery device (ERD), in order to recover energy from the pressurized flow of the diluted draw effluent, without which such a power generation process is ineffective. Moreover, the ERD in conventional PRO is expected to operate with exceptionally high overall efficiency, in order to make the process economically feasible. Recent reports [25,26] describe a new method for PRO power generation in closed circuit (PRO-CC), which entirely circumvents the need for ERD and allow such a process to proceed with near absolute energy retention efficiency. Since energy conservation in PRO hydroelectric power generation systems is a crucial issue, the new CC-PRO technology is expected to open the door for large-scale economical applications of this noteworthy approach to clean energy generation worldwide.

2. PRO membranes performance projections

A typical PRO module with an advanced membrane according to the schematic design displayed in Fig. 1 comprises a non-pressurized section and pressurized section with the former fed at inlet by a low salinity feed (LSF) with Low salinity concentrate (LSC) effluent removed from its outlet and the latter fed by a high salinity feed (HSF) at inlet with high salinity diluted feed (HSDF) removed from its outlet. LSF is commonly referred to as "feed" solution and HSF as "draw" solution. The two sections are separated by a membrane, which comprises a porous support (PS) and with a semipermeable AL. The majority of current studies in this area focus on the evaluation of the actual flux and power density of PRO membranes from theoretical models on the basis of permeability coefficients (A), salt diffusion coefficients (B), and structural parameters (S) with or without experimental results to validate the projections. The performance complexity of the PRO membrane arises from the stationary state conditions in the pressurized and non-pressurized bulk suctions of the module, which differ from those in the PS and give rise to strong ICP effects on flux.

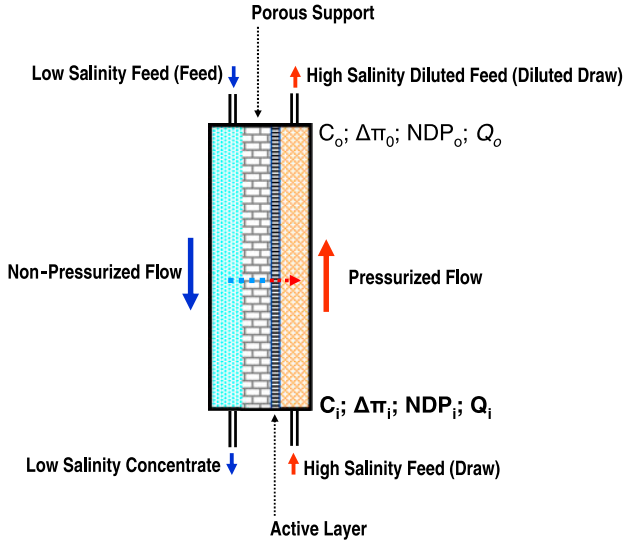

Fig. 1. Schematic illustration of a typical PRO module with its TFC membrane comprising a porous support and an AL—module pressurized section is indicated by red and non-pressurized section by blue.

The permeation flux in the pressurized section of the PRO module displayed in Fig. 1 is the source of power by this technique and irrespective whether flux decline inside the PRO module takes place uniformly or not, the undisputed performance features of such a module are as follows:

(1) The concentration (C_i), the osmotic pressure difference ($\Delta\pi_i$), and flow (Q_i) at the inlet to the pressurized section in the module are fixed and independent of applied pressure (p_a), which only affects the net driving pressure term NDP_i [$=\Delta\pi_i - p_a$]. Ideal water flux at module inlet under zero applied pressure conditions according Eq. (2) is defined by the fixed product $A \times \Delta\pi_i$.

(2) The concentration (C_o), the osmotic pressure difference ($\Delta\pi_o$), and flow (Q_o) at outlet of the pressurized section in the module are different from the fixed inlet parameters with $C_o < C_i$, $\Delta\pi_o < \Delta\pi_i$, $Q_o > Q_i$, and $NDP_i > NDP_o$, and the differences manifest the applied pressure effect on NDP and the water flux.

(3) Power availability of a PRO module is the product of $(Q_o - Q_i) \times p_a$ or $Q_p \times p_a$, where Q_p stands for the permeation flow determined by the average flux in the module with ideal power density expressed by Eq. (1).

(4) The applied pressure of ideal peak power density expected in a PRO module may be obtained by differentiating the power expression $A \times (\Delta\pi - p_a) \times p_a$ derived from Eq. (1) and Eq. (2) with respect to p_a, which yields [4] maximum when $p_a = \Delta\pi_i/2$.

The meaning of the aforementioned is that performance characterization of a PRO module requires the knowledge of both inlet and outlet parameters, and the use of inlet parameters only may suggest performance

under unrealistic conditions of exceptionally low average permeation flux, where outlet parameters differ only by little from the inlet parameters as would be expected under experimental conditions with high flow ratio of draw/permeate, which are of little practical use for a real PRO application.

In spite of the cited theoretical limitations, the knowledge of detrimental effects on flux in PRO membranes is of an important issue for the fabrication of better membranes of lower detrimental effects and higher peak power density, and this prompted the current study. Some of the reported theoretical model studies of PRO membranes on the basis of the A, B, and S include curves of ideal and actual flux as function of applied pressures which reveal near linear relationships, especially in the region of zero to maximum power density. This may suggest that a single coefficient of actual/ideal flux ratio (henceforth "β") manifests the overall detrimental effects of different origin in the same membrane and salinity gradient irrespective of the stationary state conditions dictated by the applied pressure. In simple terms, the actual water flux (J_{wa}) across the AL of the semipermeable membrane and actual power density (P_a) could be estimated by the respective expression Eqs. (5) and (6) from A and β, if the latter is a genuine representative of the combined detrimental effects. In order to ascertain the validity of the aforementioned deceptively simple approach for actual flux and power density projections of PRO membranes by means of β and A according to Eqs. (5) and (6), reported experimental data of flux at zero applied pressure for certain PRO-TFC membranes was used to generate β and actual flux and power density performance curves as well as peak power on the basis of β with results compared with relevant information obtained by rigorous theoretical models calculations and experimental data when made available. The results obtained by the β-A approach for PRO membranes performance projections are described and discussed hereinafter.

$$J_{wa} = \beta \times A \times (\Delta\pi - p_a) \tag{5}$$

$$P_a = (1/36) \times \beta \times A \times (\Delta\pi - p_a) \times p_a \tag{6}$$

2.1. MP#1 TFC-PRO membrane performance projections in SW-RW-like salinity gradient by the β-A approach

Recently, Yip et al. reported [17] a comprehensive study describing the performance of a newly prepared TFC-PRO membrane of $A = 5.81$ lmh/bar, $B = 0.88$ lmh, and $S = 349$ μm with theoretical peak power density at 10 W/m^2 in the salinity gradient system of the approximate 0.55 M–0.96 mM NaCl concentrations.

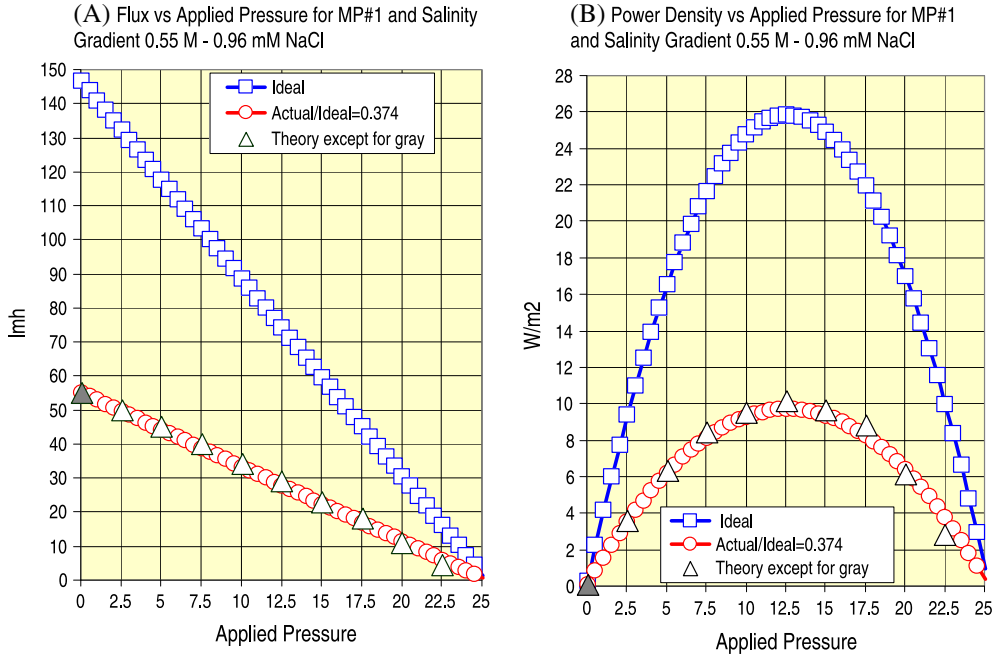

Fig. 2. The β-A (0.374 ratio and 5.81 lmh/bar) projected flux (A) and power density (B) for the TFC-PRO membrane MP#1 in the SW-RW-like salinity gradient system as compared with the reported [17] theoretical curves on the basis of $A = 5.81$ lmh/bar, $B = 0.88$ lmh, and $S = 349$ μm—the gray triangle is the experimental data that was used to determine β.

The only experimental data provided in the report was that of the actual flux at zero applied pressure (~55 bar). Data extracted from the expanded theoretical curves of flux and power density of said report [17] at the applied pressure points 0.0; 2.5; 5.0; 7.5; 10.0; 12.5; 15.0; 17.5; 20.0; and 25.0 bar are 55(0.00); 50 (3.47); 45(6.25); 40(8.33); 34(9.44); 29(10.0); 23(9.58); 18 (9.75); 11(6.11); 4.5(2.81), and 0.0 lmh (0.0 W/m^2), respectively.

The β-A based PRO projections of flux (Fig. 2(A)) and power density (Fig. 2(B)) make use of $\beta = 0.374$ determined from the reported [17] experimental flux at zero applied pressure (55 bar), and $A = 5.81$ lmh/bar according to Eq. (5). The data in Fig. 2 also includes selected reference points of the reported [17] theoretical curves on the basis of A, B, and S parameters.

2.2. PA-PES TFC-PRO membrane performance projections in SWB (0.50 M NaCl) and RW (10 mM NaCl) salinity gradient by the β-A approach

Recently, Chou et al. reported [19] a comprehensive study describing the performance of a newly prepared TFC-PRO hollow-fiber membrane of $A = 3.32$ lmh/bar, $B = 0.139$ lmh, and $S = 460$ μm with a theoretical peak power of ~9 W/m^2 at ~14 bar applied pressure in the salinity gradient system of 0.50 M–10 mM NaCl concentrations. Experimental flux and power density extracted from expanded curves in the reported data [19] at the applied pressures 0.0; 1.5; 2.5; 3.5, and 5.0 bar are 39.5(0.00); 39.0(1.63); 35.0(2.43); 34(3.31), and 33 lmh (4.58 W/m^2), respectively.

The β-A based PRO projections of flux (Fig. 3(A)) and power density (Fig. 3(B)) make use of $\beta = 0.519$ determined from the reported [19] experimental flux at zero applied pressure (39.5 lmh), and $A = 3.32$ lmh/bar according to Eq. (5). The data in Fig. 3 also includes several experimentally determined flux and power density values.

2.3. PA-PES TFC-PRO membrane performance projections in SWB (0.75 M NaCl) and RW (10 mM NaCl) salinity gradient by the β-A approach

Chou et al. also reported [19] the performance of a newly prepared TFC-PRO hollow-fiber membrane of $A = 3.32$ lmh/bar, $B = 0.139$ lmh and $S = 460$ μm with a theoretical peak power ~18 W/m^2 at ~23 bar applied pressure in the salinity gradient system of 0.75 M–10 mM NaCl concentrations. Experimental flux and power density extracted from expanded curves in the reported data [19] at the applied pressures 0.0; 1.5; 2.5; 3.5 and 5.0 bar are 46.0(0.00); 43.0(1.83); 39.5(2.96); 39(4.02) and 38.5 lmh (5.47 W/m^2), respectively.

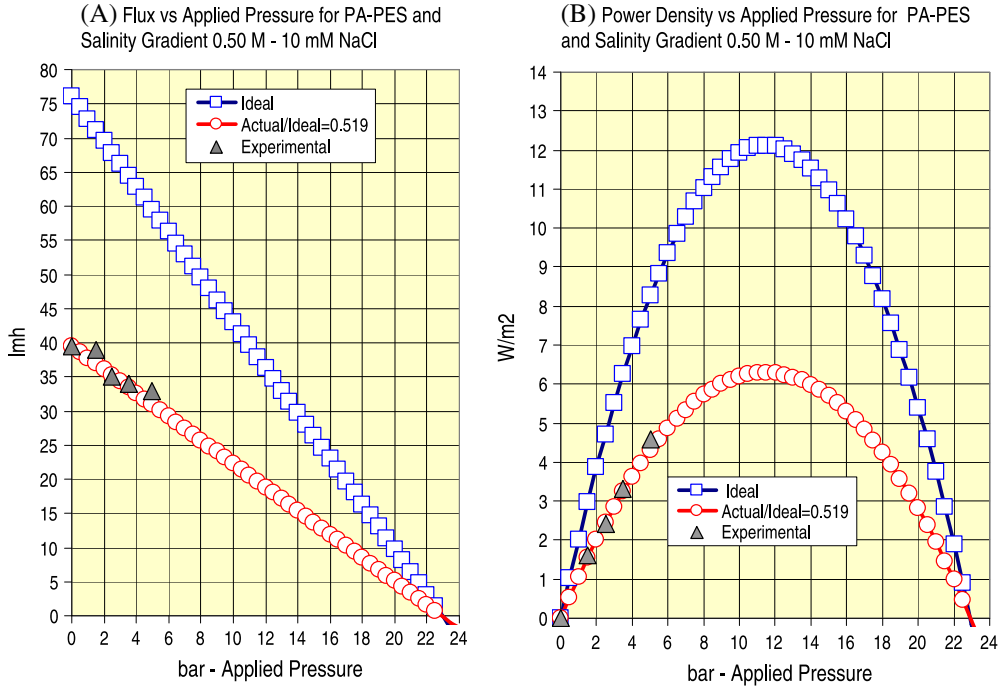

Fig. 3. The β-A (0.519 ratio and 3.32 lmh/bar [19]) projected flux (A) and power density (B) for the TFC-PRO membrane PA-PES in the SW-RW-like salinity gradient system as compared with the several reported [19] experimental data points.

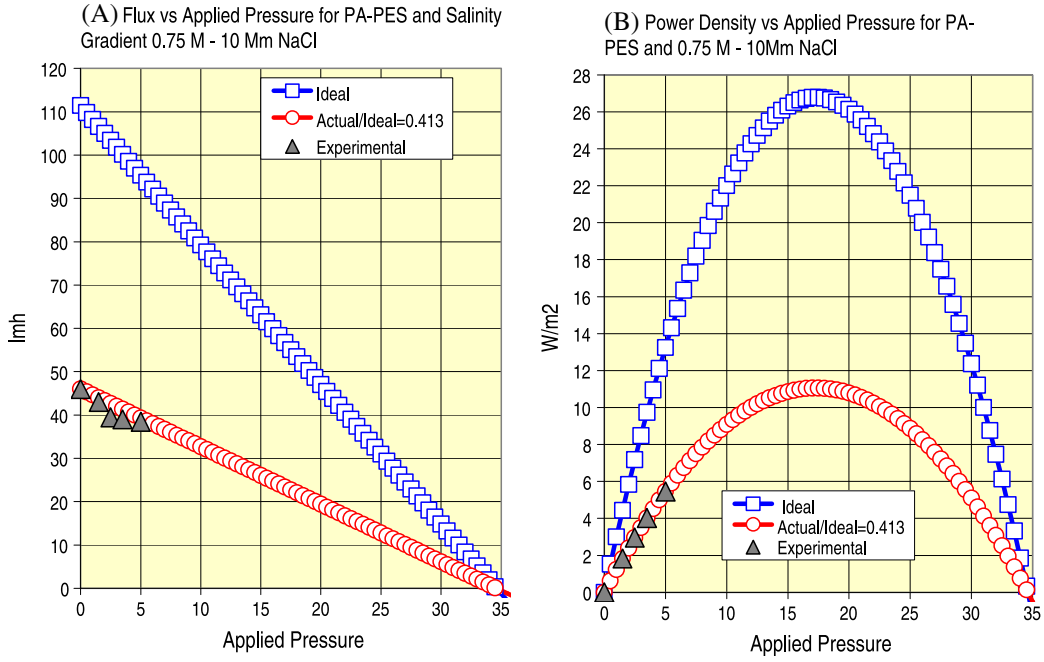

Fig. 4. The *β-A* (0.413 ratio and 3.32 lmh/bar [19]) projected flux (A) and power density (B) for the TFC-PRO membrane PA-PES in the SW-RW-like salinity gradient system as compared with the several reported [19] experimental data points.

The *β-A* based PRO projections of flux (Fig. 4(A)) and power density (Fig. 4(B)) make use of $\beta = 0.413$ determined from the reported [19] experimental flux at zero applied pressure (46.0 lmh) and $A = 3.32$ lmh/bar according to Eq. (5). The data in Fig. 4 also includes several experimentally determined flux and power density values.

2.4. PA-PES TFC-PRO membrane performance projections in SWB (1.0 M NaCl) and RW (10 mM NaCl) salinity gradient by the β-A approach

Chou et al. also reported [19] the performance of the newly prepared TFC-PRO hollow-fiber membrane of $A = 3.32$ lmh/bar, $B = 0.139$ lmh, and $S = 460$ μm with a theoretical peak power of ~28 W/m^2 at ~31 bar applied pressure in the salinity gradient system of 1.00 M–10 mM NaCl concentrations. Experimental flux and power density extracted from expanded curves of the reported [19] data at the applied pressures 0.0; 1.0; 2.5; 3.5; 6.0, and 8.0 bar are 51.5(0.00); 51.0(1.42); 50.0 (3.47); 49(4.76); 48.5(8.08), and 47 lmh (10.44 W/m^2), respectively.

The *β-A* based PRO projections of flux (Fig. 5(A)) and power density (Fig. 5(B)) make use of $\beta = 0.335$ determined from the reported [19] experimental flux at zero applied pressure (51.5 lmh), and $A = 3.32$ lmh/bar according to Eq. (5). The data in Fig. 5 also includes several reported [19] experimental data points of flux and power density.

2.5. PES-B TFC-PRO membrane performance projections in SWB (1.0 M NaCl) and RW (0.0 M NaCl) salinity gradient by the β-A approach

The very recently reported [20] study by Zhang et al. describes the performance of some newly prepared PES TFC-PRO hollow-fiber membranes of relatively high mechanical strength to withstand applied pressure up to 23 bar with a theoretical peak power of ~28 W/m^2 at ~28 bar applied pressure. The PES-B membrane, in said study, was characterized by $A = 3.30$ lmh/bar, $B = 0.31$ lmh, and $S = 450$ μm, and its testing with the 1.0 M NaCl and deionized water (0.0 M NaCl) salinity gradient system gave the experimental flux values as function of applied pressures (in parenthesis) of 69(0.0); 60 (5.5); 54(10); 48(15.5); 47(18), and 46 lmh (20 bar) and their respective power densities of 0.00; 9.30; 15.07; 19.87; 21.23, and 21.95 W/m^2 - experimental data cited here in above are estimates from expanded curves in said study [20].

The *β-A*-based PRO projections of flux (Fig. 6(A)) and power density (Fig. 6(B)) make use of $\beta = 0.447$ determined from the reported [20] experimental flux at zero applied pressure (69 lmh), and $A = 3.30$ lmh/bar according to Eq. (5). The data in Fig. 6 also includes

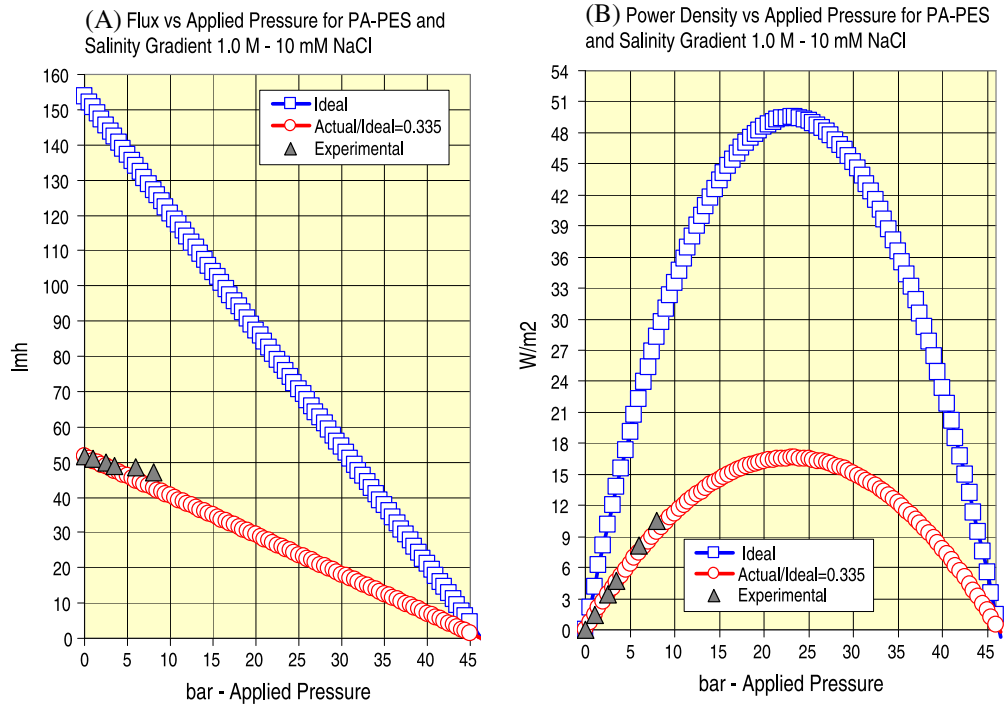

Fig. 5. The *β-A* (0.335 ratio and 3.32 lmh/bar [19]) projected flux (A) and power density (B) for the TFC-PRO membrane PA-PES in the SWB-RW-like salinity gradient system as compared with the several reported [19] experimental data points.

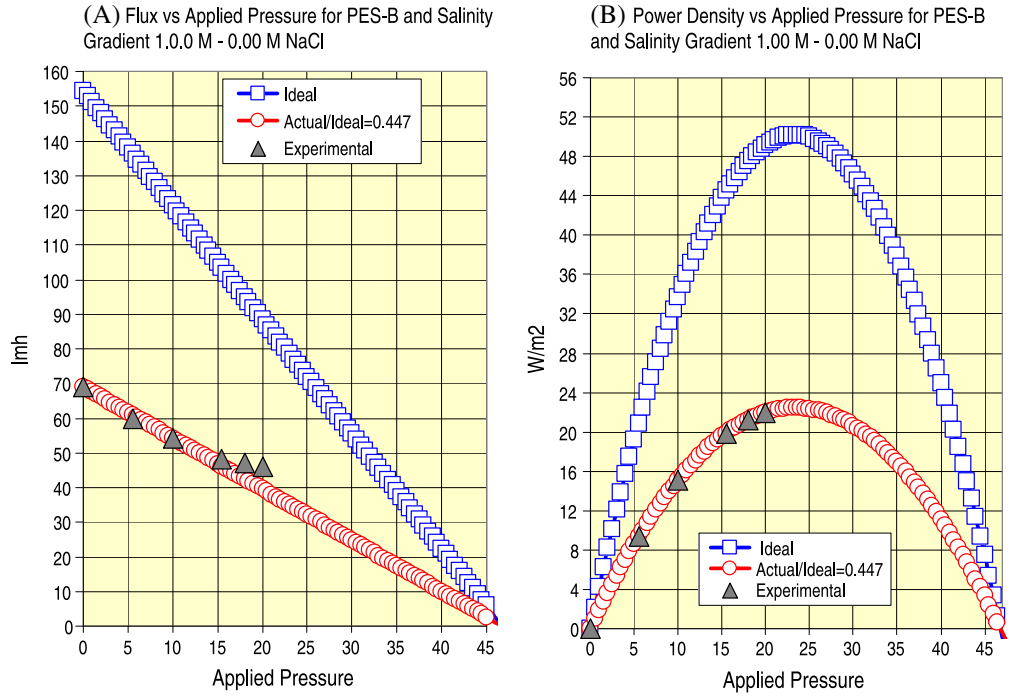

Fig. 6. The *β-A* (0.447 ratio and 3.30 lmh/bar [20]) projected flux (A) and power density (B) for the TFC-PRO membrane PES-B in the SWB-RW-like salinity gradient system as compared with several reported [20] experimental data points.

several reported [20] experimental data points of flux and power density.

2.6. PES-A TFC-PRO membrane performance projections in SWB (1.0 M NaCl) and RW (0.0 M NaCl) salinity gradient by the β-A approach

The very recently reported [20] study by Zhang et al. also describes the performance of the newly prepared PES-A TFC-PRO hollow-fiber membrane of $A = 4.0$ lmh/bar, $B = 1.65$ lmh, and $S = 550$ μm with a theoretical peak power of ~24 W/m^2 at ~24 bar applied pressure in 1.0 M NaCl and deionized water (0.0 M NaCl) salinity gradient system. This membrane gave the experimental flux values 67 (0.0); 52 (6.5); 41(10.5); 35(15.0); and 32 lmh (17.5 bar) at the cited applied pressures (in parenthesis), which correspond to power density of 0.00; 10.42; 14.63; 18.97, and 20.39 W/m^2, respectively—experimental data cited hereinabove are estimates from expanded curves in said study [20].

The β-A based PRO projections of flux (Fig. 7(A)) and power density (Fig. 7(B)) make use of $\beta = 0.358$ determined from the reported [20] experimental flux at zero applied pressure (67 lmh), and $A = 4.0$ lmh/bar according to Eq. (5). The data in Fig. 7 also includes several reported [20] experimental data points of flux and power density.

3. Discussion

The data displayed in Figs. 2–7 reveals that PRO flux and power density projections of specific membranes in defined salinity gradient systems can be generated by the knowledge of the permeability coefficient (A) and the actual/ideal flux ratio (β) at zero applied pressure. The β ratio is derived from the permeability coefficient (A), measured flux at zero applied pressure under typical conditions of FO, and ideal flux derived by Eq. (2). The application of β to ideal flux terms as a function of applied pressures according to Eq. (5) enables to establish the actual and ideal flux curves for a specific membrane in a defined salinity gradient over the entire applied pressure range as well as the respective power density terms, wherefrom peak power density is attainable. The theoretical flux and power density projection curves by the β-A approach over the entire applied pressure range for several noteworthy advance TFC-PRO membranes in various salinity gradients are provided in Figs. 2–7 together with reported experimental data. Peak power density projections reported for several noteworthy TFC-PRO membranes and those derived by the β-A method are furnished and compared in Table 1.

The draw concentration effect on β for the same membrane are evident from the data in Table 1 for PA-PES at 0.5, 0.75, and 1.0 M with β values of 0.519,

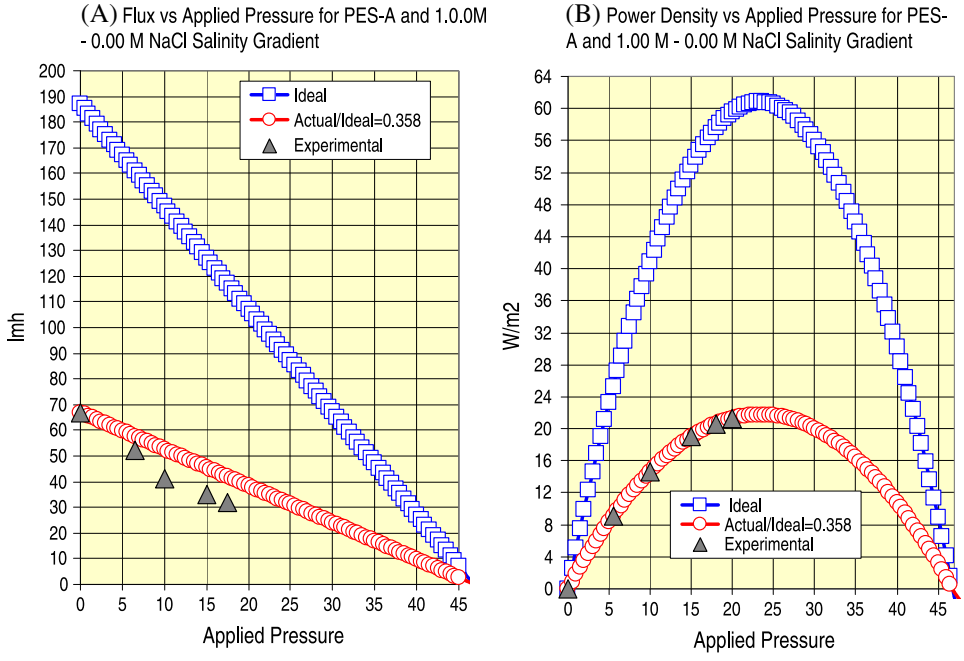

Fig. 7. The β-A (0.358 ratio and 4.00 lmh/bar [20]) projected flux (A) and power density (B) for the TFC-PRO membrane PES-A in the SWB-RW-like salinity gradient system as compared with several reported [20] experimental data points.

Table 1
Reported applied pressure peak power theoretical projections for several noteworthy TFC-PRO advanced membranes in defined salinity gradients compared with generated data by the β-A approach—the cited "Theory Peak" power density and flux information was abstracted from expanded reported curves and the term DI stands for deionized water

TFC-PRO membrane	Parameters			NaCl solutions		Theory Peak Projections			Actual/ideal flux ratio Peak Projections			$A \times \beta$
	A (lmh/bar)	B (lmh)	S (μm)	Draw (M)	Feed (mM)	(W/m2)	(bar)	Ref.	(β)	(W/m2)	(bar)	(lmh/bar)
MP#1	5.81	0.88	349	0.55	0.96	10	13	[17]	0.374	10.0	13	2.173
PA-PES	3.32	0.14	460	0.50	10	9	14	[19]	0.519	6.3	11	1.723
PA-PES	3.32	0.14	460	0.75	10	18	23	[19]	0.413	11.0	17	1.371
PA-PES	3.32	0.14	460	1.00	10	28	31	[19]	0.335	17.0	23	1.112
PES-B	3.30	0.31	450	1.00	0(DI)	28	28	[20]	0.447	23.0	24	1.475
PSE-A	4.00	1.16	450	1.00	0(DI)	24	24	[20]	0.358	22.0	23	1.432

0.413, and 0.335 corresponding to 6.3, 11, and 17 W/m^2 peak power density at 11, 17, and 23 bar applied pressures, respectively. The aforementioned data revealed in Fig. 8(A)–(C) near linear relationships between β and peak power density (Fig. 8(A)), applied pressure at peak power (Fig. 8(B)) and draw salinity concentration (Fig. 8(C)). The noteworthy peak power difference between MP#1(10 W/m^2; $\beta = 0.384$; 0.55 M) and PA-PES (6.3 W/m^2; $\beta = 0.519$; 0.50 M) for similar draw concentrations most probably reflects the dominant effect of the permeability coefficient (A), and the lesser relative effect of salt diffusion coefficient (B) on peak power generation of PRO membranes. In this context, noteworthy is the product $A \times \beta$, which according to Eq. (5) signifies the effective permeability coefficient of given membranes in a defined salinity gradient system, or in simple terms, the effectiveness of the PRO membrane for power generation application. The $A \times \beta$ value of MP#1(2.173) as compared with that of PA-PES (1.723) for draw of similar concentrations clearly explain the greater effectiveness of the former membrane. Likewise, the decreased $A \times \beta$ product values in the PA-PES series as a function of increased draw concentration most probably suggests the declined effectiveness of the membrane for PRO power generation due to increased detrimental effects as result of increased reverse salt flux.

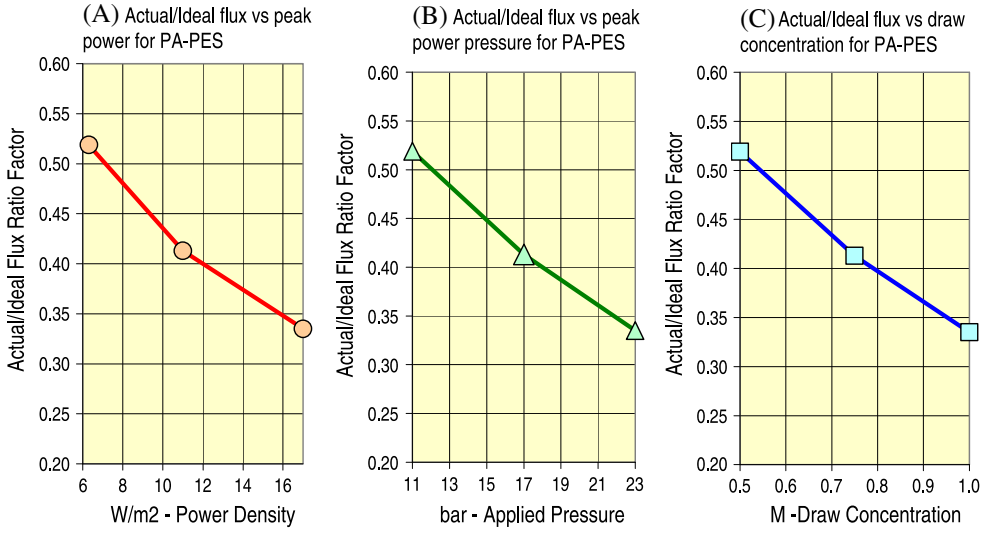

Fig. 8. The relationships between β and peak power density (A), applied pressure at peak power (B), and draw salinity concentration 8(C) for the PA-PES membrane according to the data in Table 1.

The general validity of the *β-A* approach for PRO power projections will be determined ultimately when more experimental peak power data on PRO membranes shall become available in the vicinity of the peak power applied pressures. Presently, the *A-β* analysis is limited to only few cases of advance membranes and with peak power extrapolated from different theoretical curves and experimental results generated mainly from laboratory-scale PRO setup systems with recycled draw and feed solutions under constantly changing conditions at the module inlet at the same applied pressure. I should be pointed out that modules in conventional PRO are engaged in a single pass-process of defined inlet and outlet parameters, and such conditions are not attained during experiments with recycled feed and draw solutions. Evidently, single-pass experimental PRO results are required in order to allow accurate comparison with theory derived projections. The theoretical curves for MP#1 [17] of high competence origin reveal (Fig. 2) near complete consistency with the *β-A* projections and the *β-A* curves for PA-PES (Figs. 3–5), PES-B (Fig. 6), and PES-A (Fig. 7) show a sufficiently good agreement with the available reported experimental results. Incidentally, reported experimental flux and power density results are commonly found below the theoretical curves and the same is also manifested by comparison with the *β-A* curves presented hereinabove.

The comparison between *β-A* extrapolated peak power and applied pressure at peak power and such data from various reported theoretical curves for the PRO membranes under review in Table 1 is

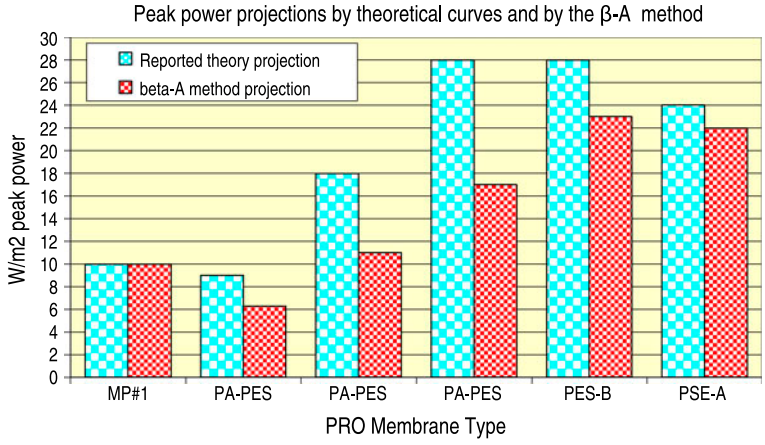

Fig. 9. Comparison of peak power projections by theoretical curves and by the *β-A* method of the certain advanced TFC-PRO membranes according to the data in Table 1.

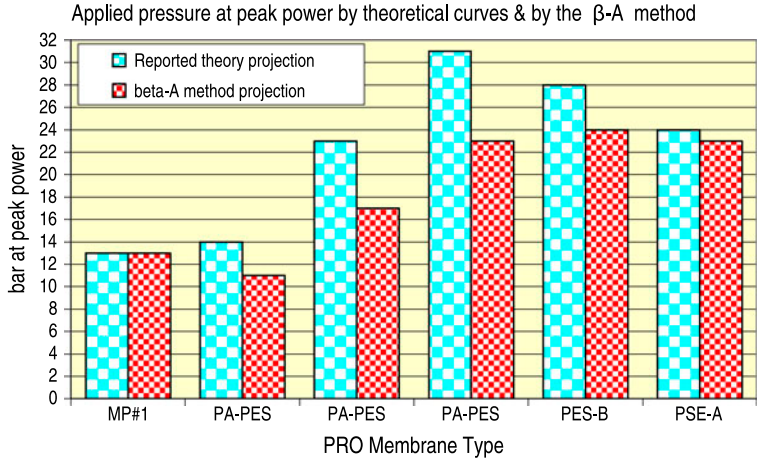

Fig. 10. Comparison applied pressure projections by theoretical curves and by the *β-A* method of the certain advanced TFC-PRO membranes according to the data in Table 1.

illustrated in Figs. 9 and 10, respectively. The data furnished Fig. 9 shows complete consistency of peak power projections for MP#1 from the reported [17] theoretical curve and by the β-A approach, and the same also true for the applied pressure of peak power displayed in Fig. 10. Peak power projections (Fig. 9) from the theoretical curves of the other PRO membranes in Table 1 are consistently higher than those derived by the β-A approach, and the same trend is also revealed for the applied pressure at peak power (Fig. 10). Some of the theory projected applied pressures at peak power are found removed from the expected mid-osmotic pressure difference of the salinity gradients and their verification should await the availability of experimental data.

References

[1] S. Loeb, Method and apparatus for generating power utilizing pressure-retarded-osmosis, US patent No. 3,906,250 1975.

[2] S. Loeb, Osmotic—Power plants, Science 189(4203) (1975) 654–655.

[3] S. Loeb, S. Sourirajan, American chemical society advances in chemistry series, ACS 38 (1963) 117–132.

[4] A. Achilli, A.E. Childress, Pressure retarded osmosis: From the vision of Sidney Loeb to the first prototype installation—Review, Desalination 261 (2010) 205–211.

[5] B.E. Logan, M. Elimelech, Membrane-based processes for sustainable power generation using water, Nature 488 (2012) 313–319.

[6] M. Elimelech, W.A. Phillip, The future of seawater desalination: Energy, technology and the environment, Science 333 (2011) 712–717.

[7] S. Loeb, Energy production at the Dead Sea by pressure-retarded osmosis: Challenge or chimera? Desalination 120 (1998) 247–262.

[8] S.E. Skilhagen, J.E. Dugstad, R.J. Aaberg, Osmostic power—power production based on the osmotic pressure difference between waters and varying salt gradients, Desalination 220 (2008) 476–482.

[9] S.E. Skilhagen, G. Brekke, W.K. Nielsen, Progress in the development of osmotic power, in: Qingdao International Conference on Desalination and Water Reuse, Proceedings, June 20–23, 2011, Qingdao, China, 247–260.

[10] G. Brekke, Review of experience with the Statkraft prototype plant, in: The 3rd Osmosis Membrane Summit, April 26–27, 2012, Barcelona, Spain.

[11] A. Tanioka, Power generation by pressure retarded osmosis using concentrated brine from seawater desalination system and treated sewage, review of experience with pilot in Japan, in: The 3rd Osmosis Membrane Summit, April 26–27, 2012, Barcelona, Spain.

[12] M. Kurihara, Government funded programs worldwide, the Japanese "Mega-ton water system" project, in: The 3rd Osmosis Membrane Summit, April 26–27, 2012, Barcelona, Spain.

[13] K. Saito, M. Irie, S. Zaitsu, H. Sakai, H. Hayashi, A. Tanioka, Retarded osmosis using concentrated brine from SWRO system and treated sewage as pure water, Desalin. Water Treat. 41(3) (2012) 114–121.

[14] J.R. McCutcheon, M. Elimelech, Influence of membrane support layer hydrophobicity on water flux in osmotically driven membrane process, J. Membr. Sci. 318 (2008) 458–466.

[15] N.Y. Yip, A. Tiraferri, W.A. Phillip, J.D. Schiffman, M. Elimelech, Performance thin-film composite forward osmosis membrane, Environ. Sci. Technol. 44 (2010) 3812–3818.

[16] N.Y. Yip, M. Elimelech, Performance limiting effects in power generation from salinity gradients by pressure retarded osmosis, Environ. Sci. Technol. 45 (2011) 10273–10282.

[17] N.Y. Yip, A. Tiraferri, W.A. Phillip, J.D. Schiffman, L.A. Hoover, Y.C. Kim, M. Elimelech, Thin-film composite pressure retarded osmosis membranes for sustainable power generation from salinity gradients, Environ. Sci. Technol. 45 (2011) 4360–4369.

[18] N.Y. Yip, M. Elimelech, Thermodynamic and energy efficiency analysis of power generation from natural salinity gradients by pressure retarded osmosis, Environ. Sci. Technol. 46 (2012) 5230–5239.

[19] S. Chou, R. Wang, L. Shi, Q. She, C. Tang, A.G. Fane, Thin-film hollow fiber membrane for pressure retarded osmosis (PRP) process with high power density, J. Membr. Sci. 389 (2012) 25–33.

[20] S. Zhang, T.S. Chung, Minimizing the instant and accumulation effects of salt permeability to sustain ultrahigh osmotic power density, Environ. Sci. Technol. 47 (2013) 10085–10092.

[21] S. Zhang, F. Fu, T.S. Chung, Substrate modified and alcohol treatment on this film composite membranes for osmotic power, Chem. Eng. Sci. 87 (2013) 40–50.

[22] X. Li, S. Zhang, F. Fu, T.S. Chung, Deformation and reinforcement of thin-film composite (TFC) polyamide-imide (PAI) membranes for osmotic power generation, J. Membr. Sci. 434 (2013) 204–217.

[23] G. Han, S Zhang, X. Li, T.S. Chung, High performance thin film composite pressure retarded osmosis (PRO) membranes for renewable salinity-gradient energy generation, J. Membr. Sci. 440 (2013) 108–121.

[24] X. Song, Z. Liu, D.D. Sun, Energy recovery from concentrated seawater brine by a thin-film nanofiber composite pressure retarded osmosis membranes with high power density, Energy Environ. Sci. 6 (2013) 1199–1210.

[25] A. Efraty, Pressure-retarded osmosis in closed circuit: A new technology for clean power generation without need of energy recovery, Desalin. Water Treat. 2013 (2013) 1–11, doi:10.1080/19443994.2013.793499.

[26] A. Efraty, Closed circuit pressure retarded osmosis—A new technology for clean power generation without need for energy recovery, in: The Third Osmosis Membrane Summit, April 26–27, 2012, Barcelona, Spain.